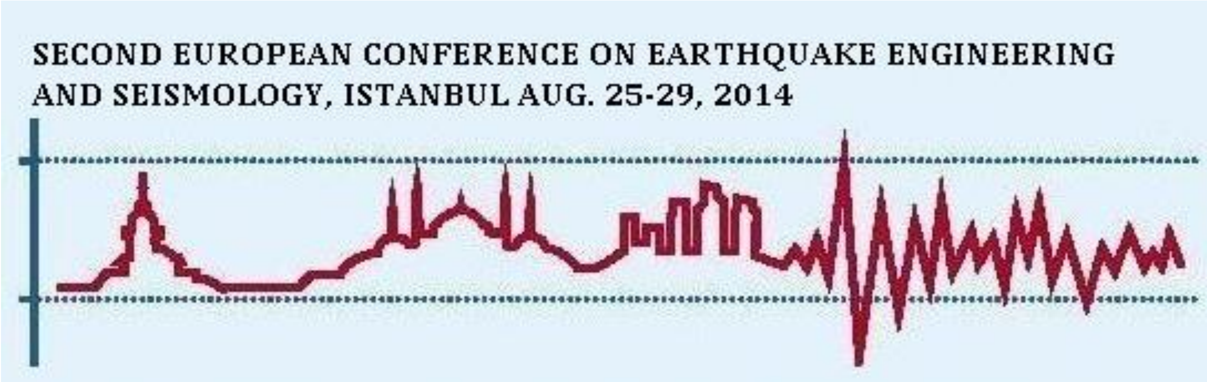

AN UPDATED HISTORY OF THE EARTHQUAKE PERFORMANCE OF A LARGE SPAN STRUCTURE

Ion VLAD[1], Horea SANDI[2], Patricia MURZEA[3], Octavia PĂUCESCU[4], Nausica VLAD[5]

ABSTRACT

A large span structure (diameter: 96 m) was built in 1961 in Bucharest in order to host the activities specific to a main exhibition, as well as to the organization of large assemblies.

The structure was subjected to date, during its service time to date of more than five decades, to several strong earthquakes: 1977.03.04 (M_{GR} = 7.2), 1986.08.30 (M_{GR} = 7.0), 1990.05.30 (M_{GR} = 6.7) and 1990.05.31 (M_{GR} = 6.3). The damage was particularly severe in 1977, but was significant also after rehabilitation and strengthening works were carried out and the 1986 event occurred, and the same happened after the 1990 events.

The importance of the structure required to perform several activities of monitoring, intervention and maintenance, relying on engineering analyses, monitoring of dynamic characteristics, investigation of damage, design of rehabilitation and strengthening solutions. Besides this, it represented an efficient tool for the calibration of a ground motion model. An accident having occurred to the initial roof structure raised also problems that deserve still to be investigated.

INTRODUCTION

The paper is devoted to the presentation of some studies that benefited from the existence, in Bucharest, of a large span structure having some peculiar, advantageous, features. The structure, presented in Figure 1, is currently in service and is managed by ROMEXPO.

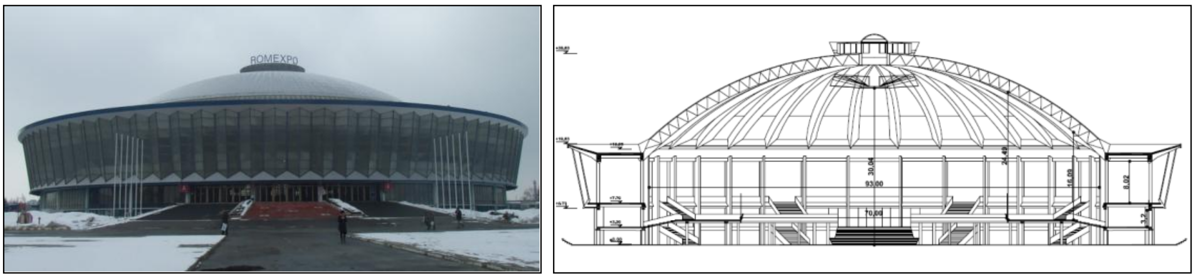

Figure 1. The main ROMEXPO exhibition hall

[1] Professor, Technical University of Civil Engineering, Bucharest, vlad@dial.kappa.ro
[2] Hon. Professor, Technical University of Civil Engineering (RNCEEV), Bucharest, horeasandi@yahoo.com
[3] Dr. Eng., ICECON S.A., Bucharest, patricia.murzea@icecon.ro
[4] Associate Professor, Technical University of Civil Engineering, Bucharest, opaucescu@utcb.ro
[5] Dr. Eng., Technical University of Civil Engineering (RNCEEV), Bucharest, vladi@itcnet.ro

In 1958 an impressive large span structure, with a reticular dome roof composed of a three-way system of steel tubes was erected in Brno, a city in former Czechoslovakia. The special roof cover of the building, designed by Prof. Ferdinand Lederer, was subject of a number of works published, especially in German language. A reference presentation in this view is provided in (Lederer, 1961) Impressed by the magnificence of that structure, known as ”Pavilion Z”, the Romanian authorities decided to build a similar structure in Bucharest, Romania, in order to serve the activity of promoting the country’s trade and economic, technical and scientific collaborative relationships.

A BRIEF HISTORY OF STRUCTURAL LIFE AND OF STUDIES UNDERTAKEN

The structure was completed in August 1961 and, for 17 months, had a good behaviour. On January 30, 1963, the dome collapsed under a strong dissymmetric snow load. This event raised some acute questions, that would have deserved in depth analyses Some first studies (Soare, 1963) have yet to be completed. .During the period that followed, the dome has been completely redesigned by a group of the Technical University of Timişoara, led by Prof. Dan Mateescu. The new design concept was totally different from that of the Brno dome. The new dome is composed of a series of 32 radial semi-arches resting on an upper compression ring and on a lower tension ring.

The structure was subjected to date, during its service time of more than five decades, to several strong earthquakes: 1977.03.04 (M_{GR} = 7.2), 1986.08.30 (M_{GR} = 7.0), 1990.05.30 (M_{GR} = 6.7) and 1990.05.31 (M_{GR} = 6.3). The damage was particularly severe in 1977, but it was also significant after rehabilitation and strengthening works were carried out and the 1986 event occurred, and the same happened after the 1990 events.

Due to the importance of the structure, several activities of monitoring, intervention and maintenance were required. These activities relied on engineering analyses, monitoring of dynamic characteristics, investigation of damage, design of rehabilitation and strengthening solutions.

Fortunately, the monitoring of dynamic characteristics had already been initiated before the destructive 1977 earthquake. This made it possible to obtain a comprehensive picture of the impact of earthquakes, as well as of the effects of intervention measures, as presented in Table 1. The experimental work, based on the recording of ambient vibration, was performed up to 1993 using an analog six–channel Soviet MIKS system (Sandi et al., 1986), and, more recently, in 2012, using a digital eight-channel American Kinemetrics system (Murzea et al., 2013a), (Murzea et al., 2013b). Using the analog MIKS system required adopting during field work alternative configurations of the recording network, i.e. adopting for the various kinds of structural deformation several series type electrical connections. The more recent use of the digital Kinemetrics system required a single configuration of the field recording network, followed by appropriate processing at home (Vlad and Vlad, 2014). The studies referred to made to possible to develop a comprehensive picture of the biography of the dynamic characteristics of the structure.

Table 1. Evolution of the Natural Periods for Various Kinds of Displacements/Deformation

Oscillation type (DOF)	Instrumental investigations stages						
	Before 1977.03.04 earthquake July, 1976	After 1977.03.04 earthquake March, 1977	After provisional strength’ng (steel bracing) April, 1977	After final strength’ng (RC spatial frame) July, 1984	After 1986.08.30 earthquake September, 1986	After 1990.05.30 earthquake July, 1993	May, 2012
N-S ring translation	0.60	1.08	0.78	0.55	0.65	0.66	0.78
E-W ring translation	0.60	0.98	0.74	0.52	0.65	0.72	0.78
In-plane ring rotation	0.41	0.94	0.59	0.43	0.52	0.52	0.75
Ring ovalization	0.35	0.36	0.36	0.34	0.39	0.41	0.39

A look at Table 1 reveals the obvious, significant, effects of successive earthquakes and of man’s interventions.

In addition to the studies referred to, the structure was used also as a tool for calibration of a stochastic model of ground microtremors. This model was proposed in 1992, with some addenda in 2005 (Sandi, 2005). The calibration attempt has been initiated in (Murzea, 2012).

Some of the studies and results, considered to be the most relevant, are presented in the paper.

MODELLING THE STRUCTURE

The structure dealt with is obviously a large size, large span, complex one. On the other hand dealing with experimental techniques requires, as always, some preparatory analytical work, relying to a high extent on specific experience, in order to provide an efficient orientation to the experimental work to be performed.

A qualitative look at the structure led to the idea that the dynamic performance of the structure as a whole (at least in the linear range) should be governed by the displacements and deformation, in its own horizontal plane, of the upper, main, ring, which directly supports at its turn the roof structure.

The almost perfect (periodic) axial symmetry of the structure made it possible to identify following categories of relevant oscillations:

- oscillations of ring rotation in a horizontal plane, with respect to the vertical symmetry axis of the structure;
- oscillations of ring ovalization of various orders:
    - of order 0: axisymmetric dilatation;
    - of order 1: rigid translation along a horizontal direction;
    - of order 2: ovalization with 2 × 2 ventra;
    - of order 3: ovalization with 2 × 3 ventra;
    - of order 4: ovalization with 2 × 4 ventra;
    - etc.

These statements were clearly confirmed by the computer analysis of the structure using the ETABS program (Murzea, 2012). To illustrate this, the displacements corresponding to some relevant natural modes are presented subsequently.

The computer model is presented in Figures 2 and 3. The most spectacular modes, for which proper ovalizations of orders 2 (first proper ovalization), 3 and 4 are well visible, are presssented in Figures 4, 5 and 6 respectively.

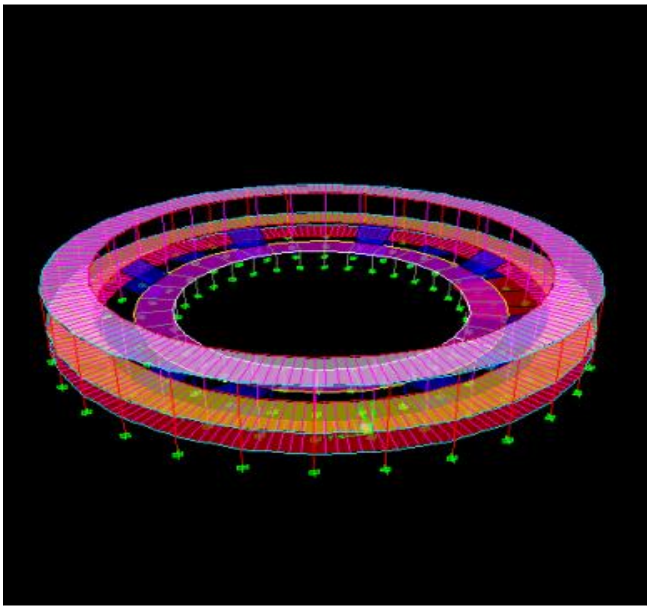

Figure 2. View of the successive rings of the ROMXPPO structure.

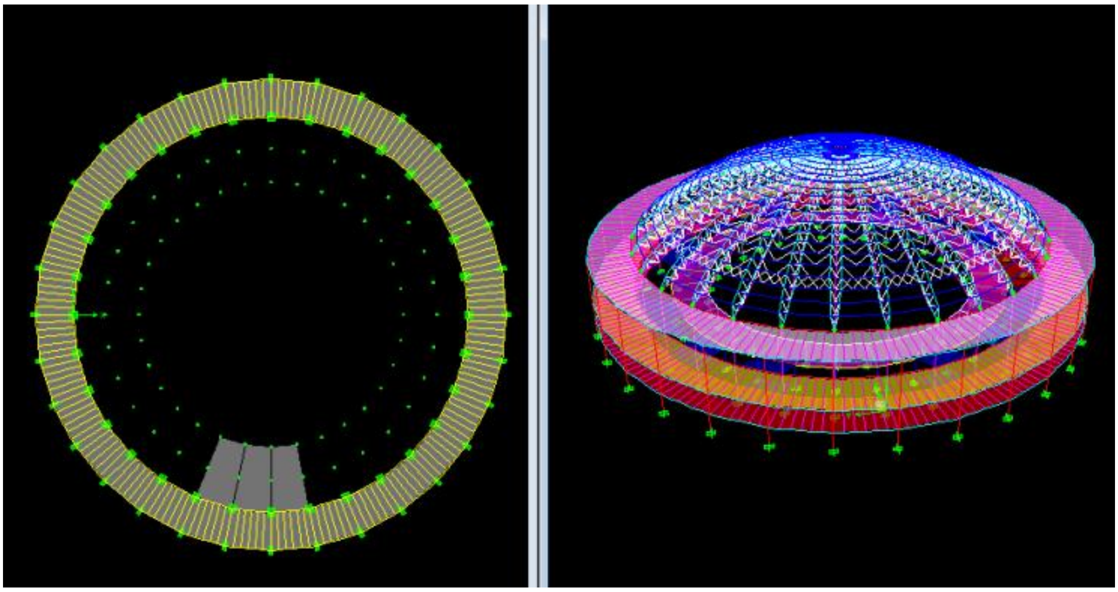

Figure 3. Model of the Central ROMEXPO Pavilion, ETABS

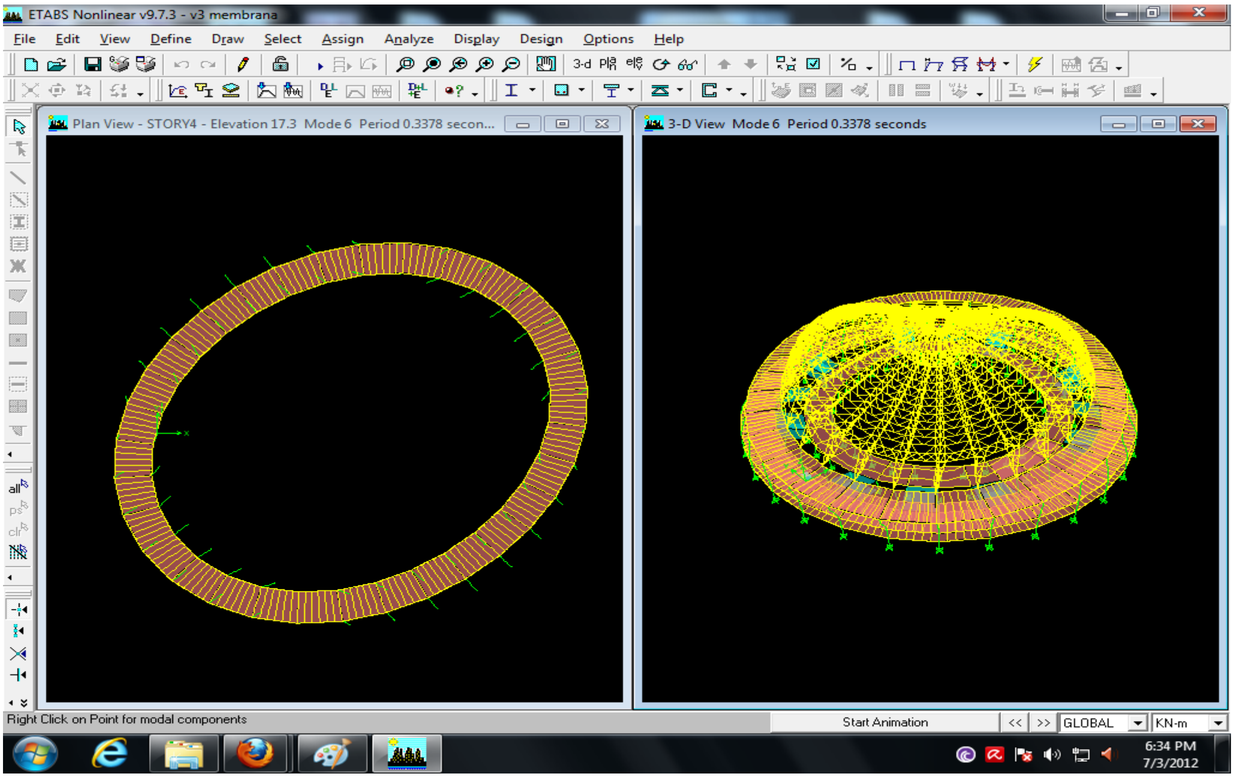

Figure 4. Horizontal ring displacements for mode 6

The lower 12 modes determined correspond respectively to: rotation of ring with respect to the central symmetry axis of the structure (mode 1), translation of ring (modes 2, 3), rotation, upper mode (mode 4), 2-nd order ovalization (modes 5, 6), upper translation (modes 7,8), 3-rd order ovalization (modes 9, 10) and 4-th order ovalization (modes 11, 12).

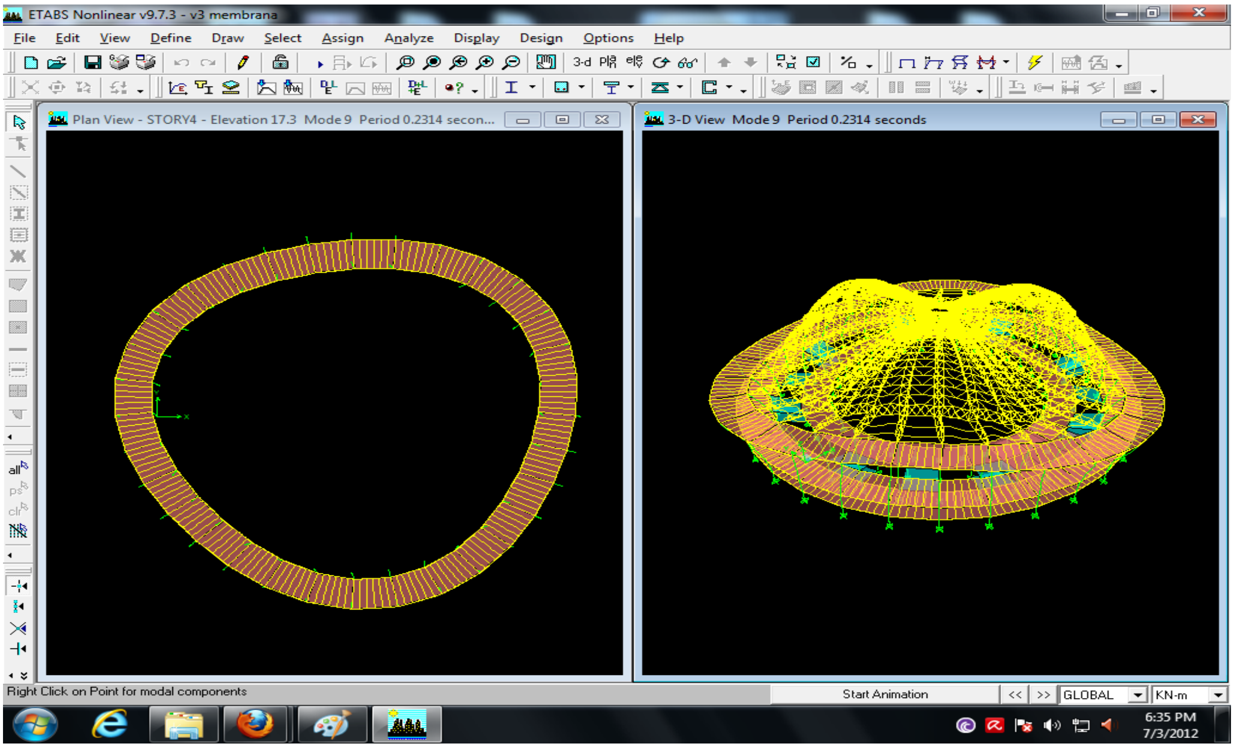

Figure 5. Horizontal ring displacements for mode 9

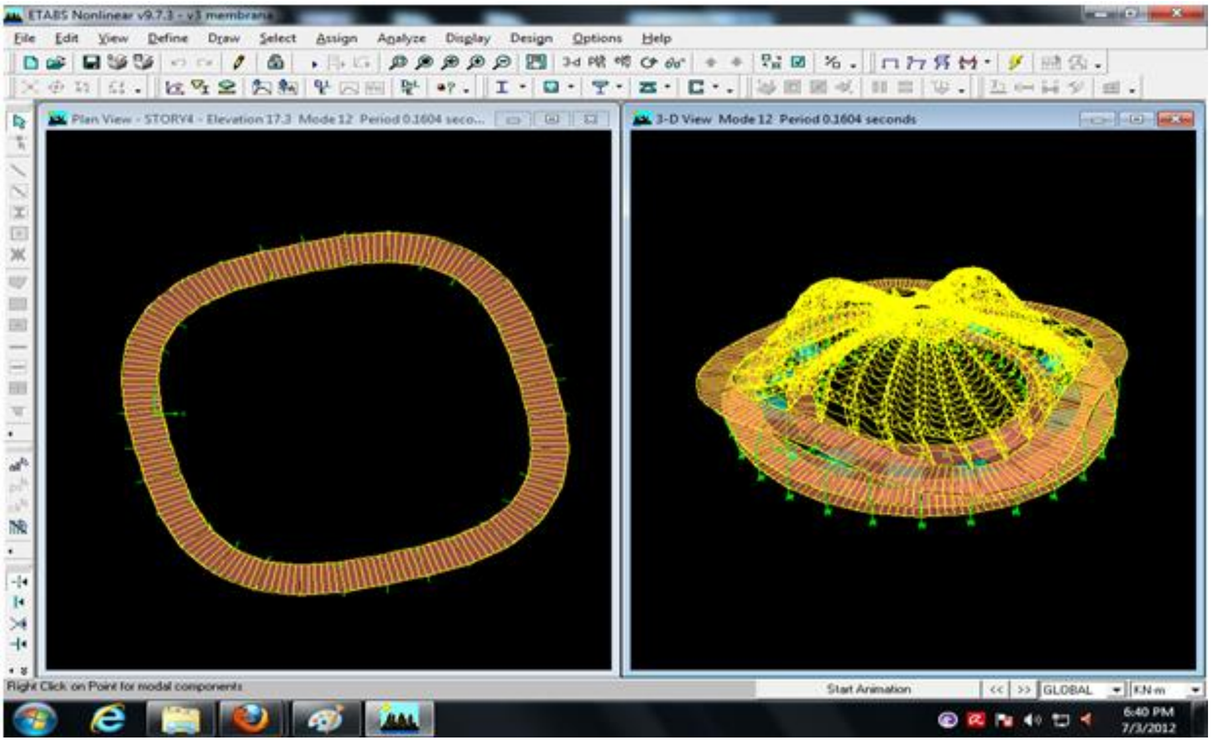

Figure 6. Horizontal ring displacements for mode 12.

METHODOLOGICAL FEATURES OF NEWLY PERFORMED EXPERIMENTAL ANALYSIS

The newly performed experimental analysis benefited from the availability of high performance digital equipment produced by Kinematrics. This made it possible to record basic signals concerning the motion at various points, along various directions, and to combine these signals subsequently, according to needs. The availability of digital signal combination and processing techniques made it possible to perform Fourier analysis and to determine, with high accuracy, several dynamic characteristics of interest.

The measuring / recording equipment available made it possible, of course, to record local motions along a limited number of degrees of freedom. Several recording schemes were imagined. It turned out that the most relevant, feasible, scheme is to place pick ups according to Figure 7.

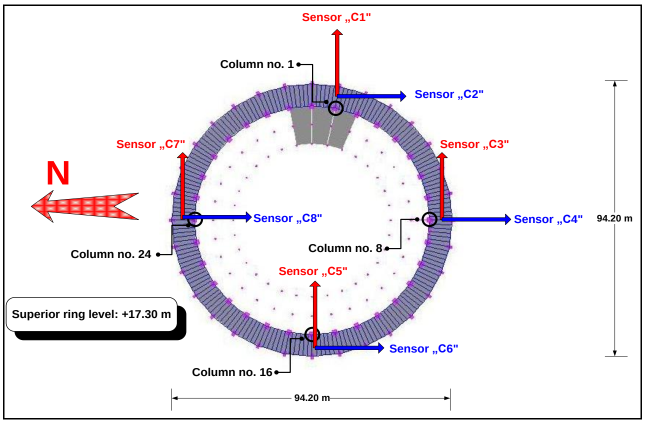

Figure 7. Placing of seismometers

The recording system produced basically time histories of velocities along the degrees of freedom put to evidence in Figure 7. These were combined according to needs and Fourier analysis of the combinations obtained on this basis was thereafter performed.

The information on Fourier amplitudes made it possible to compare the outcome for different kinds of oscillations (as referred to previously). Looking at the expressions characterizing the stochastic ground motion model presented in Annex I, it was possible to estimate the most likely values of the parameters c_p and c_s (conventional values of wave propagation speeds characterizing the ground motion model).

Rather for illustration, some possible combinations of basic time histories of records are given:

- for rotation in a horizontal plane:

$$u_{rot} = (u_3 - u_2 - u_7 + u_6)/4 \quad (1)$$

- for ovalization of order 0 (dilatation):

$$u_{dil} = (u_1 + u_4 - u_5 - u_8)/4 \quad (2)$$

- for ovalization of order 1 (N-S translation):

$$u_{NS} = (u_2 + u_4 + u_6 + u_8)/4 \quad (3)$$

- for ovalization of order 2 (proper ovalization of lowest order):

$$u_{ov2} = (u_4 - u_1 - u_8 + u_5)/4 \quad (4)$$

MAIN RESULTS OBTAINED

The basic instrumental information obtained is represented by the time histories of motion along the degrees of freedom specified in Figure. 8. A fragment of the time histories of displacements and of velocities is given, for illustration, in Fig. 8.

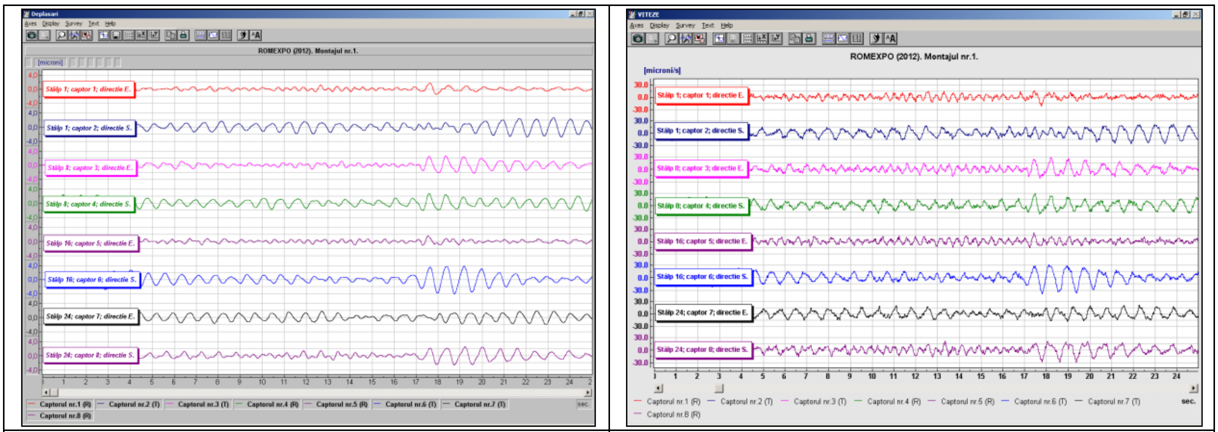

Displacements	Velocities

Figure 8. Time histories along the basic degrees of freedom

Keeping in view the structural symmetry, the records of motion along the basic degrees of freedom were combined according to equations (1), (3) and (4), in order to obtain results expected to be significant for the most relevant normal modes of the structure. Following figures present in this connection the time histories of combined velocities for the most relevant normal modes as well as the corresponding amplitude Fourier spectra.

For oscillations of rotation with respect to the vertical symmetry axis of the structure one has the outcome of Figure 9.

For oscillations of translation along the NS direction one has the outcome of Figure 10.

For oscillations of lowest order (order 2) ovalization one has the outcome of Figure 11.

A look at the time histories presented in the left halves of Figures 9,10 and 11 reveals the fact that these time histories are almost sinusoidal. This fact led to the consequence of particularly strong spectral peaks, put to evidence in the corresponding right halves of the figures.

The oscillation frequencies (and periods) corresponding to the peaks referred to are summarized in Table 2.

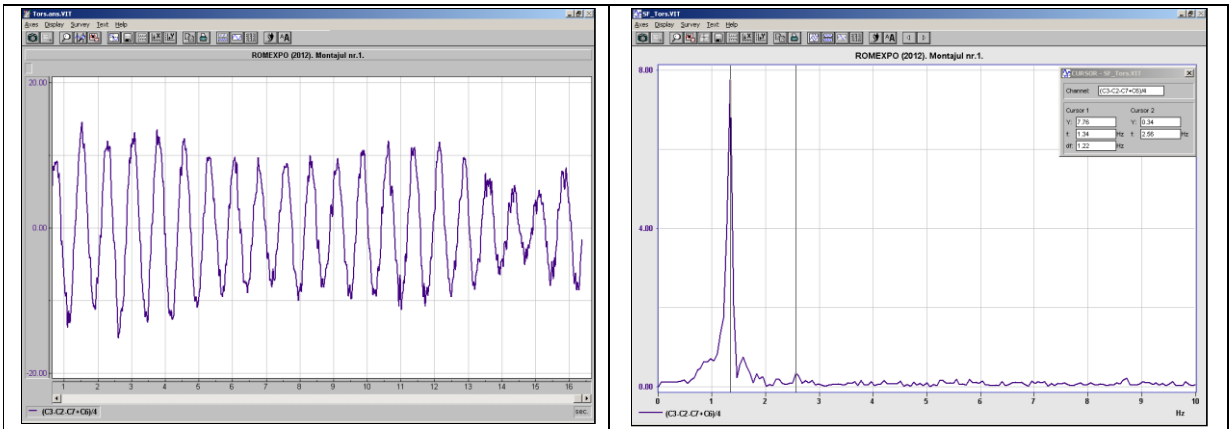

Time history of velocity	Amplitude Fourier spectrum of velocity

Figure 9. Oscillations of rotation with respect to the vertical symmetry axis of the structure

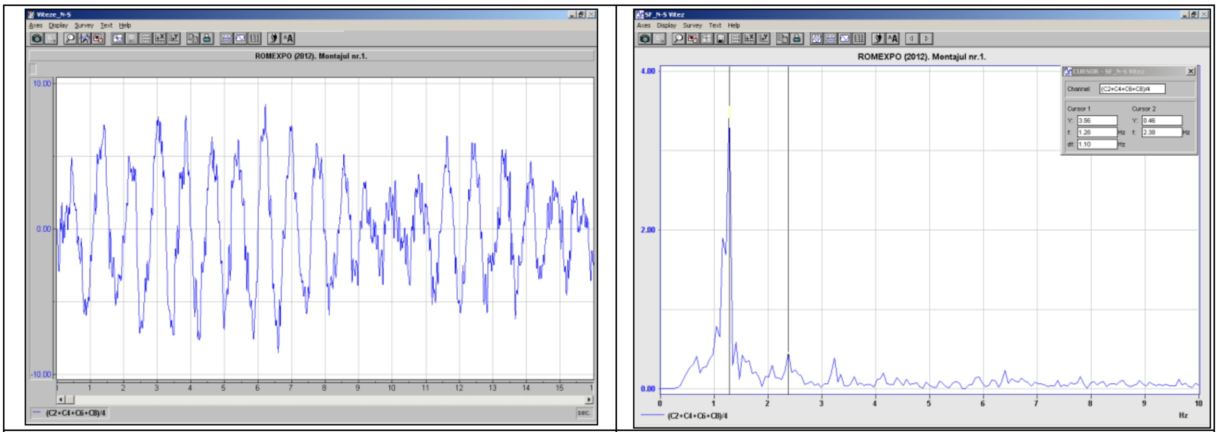

Time history of velocity	Amplitude Fourier spectrum of velocity

Figure 10. Oscillations of translation along the NS direction

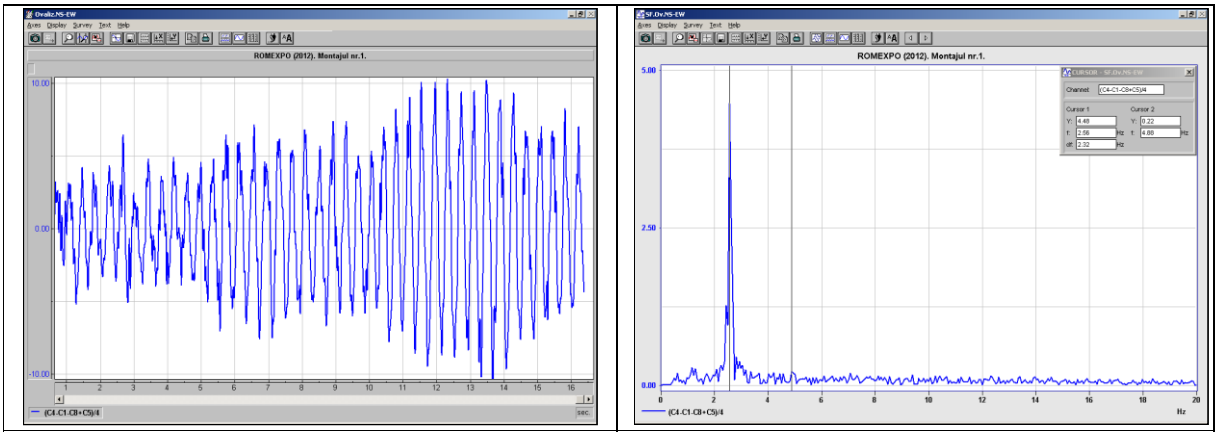

Time history of velocity	Amplitude Fourier spectrum of velocity

Figure 11. Oscillations of lowest order (2) proper ovalization

Using the methodological developments presented at the end of previous section, for ratios $a_r[\mathbf{w}_e;\ \omega]$ corresponding alternatively to displacements and velocities, it turned out that a reasonable estimate of parameters c_p and c_s is in the range of c_p = 400 m/s and c_s = 250 m/s (see also Annex II)..

Table 2. Frequencies and Periods Corresponding to the Modal Oscillations

Type of oscillation	Frequency (Hz)	Period (s)	Spectral peak, displacements	Spectral peaks, velocities
Rotation with respect to symmetry axis	1.34	0.746	0.52	4.2
Translation, NS direction	1.28	0.781	0.35	2.8
Translation, EW direction	1.28	0.781	0.32	3.2
Lowest order (2) proper ovalization	2.56	0.391	0.42	7.2

FINAL CONSIDERATIONS

It may be stated that the existence of the ROMEXPO structure dealt with in the paper represented an excellent opportunity for organizing research activities of a quite wide profile. These activities were oriented either to the investigation of problems concerning the structure, or of problems for which the existence of the structure as a tool was beneficial.

The structural model identification undertaken confirmed the governing role of the displacements and deformation of the upper ring in its horizontal plane. He categories of oscillations anticipated were strongly confirmed by rhe peaks of the Fourier amplitude spectra computed. The history of natural periods offered a quite clear basis for the estimate of damage severity and of efficiency of rehabilitation and strengthening works.

On the other hand, the availability of the data concerning the structural characteristics offered a good opportunity for the calibration of the stochastic ground motion model proposed. This latter outcome is of interest for specifying the features of spatial seismic action for various categories of structures.

ANNEX I. MAIN FEATURES OF THE GROUND MOTION MODEL PROPOSED

The model proposed concerns the motion of a half-space of a classical continuum, related to the orthogonal Cartesian axes *x*, *y* (horizontal) and *z* (vertical). The half-space may consist of a sequence (even continuous) of constant thickness, parallel, horizontal, isotropic and homogeneous layers. The local motion is characterized by three translation components, *u*, *v* and *w*, and by three rotation components of a horizontal elementary facet, $\varphi = \partial w / \partial x$, $\chi = \partial w / \partial y$ and $\psi = (\partial v / \partial x - \partial u / \partial y) / 2$ respectively (Sandi, 1983). The components referred to build together a vector $\boldsymbol{u}_g(P, t)$**,** having a transpose

$$\boldsymbol{u}_g^T(P,t) = [u(P,t), v(P,t), w(P,t), \chi(P,t), -\varphi(P,t), \psi(P,t)] \tag{5}$$

where *P* represents a point of coordinates (*x*, *y*, *z*).

The ground motion is assumed (Sandi, 2005) to be random, homogeneous with respect to the horizontal axes and stationary. Its basic characteristic is the coherence matrix $S\,[\boldsymbol{w_g};\ \omega, \Delta x, \Delta y, z_0]$ of the acceleration vector $\boldsymbol{w}_g(P,\ t)$ corresponding to the displacement vector $\boldsymbol{u}_g(P,\ t)$. The coherence matrix concerns the motion at two points P_1 and P_2, located at a same depth z_0 and at a relative position in the horizontal plane defined by the components Δx and Δy.

The isotropy and homogeneity assumptions mentioned lead to the conditions

$$s_{12} = s_{13} = s_{21} = s_{23} = s_{31} = s_{32} = s_{14} = s_{15} = s_{24} = s_{25} = s_{36} = s_{41} = s_{42} = s_{46} = s_{51} = s_{52} = s_{56} = s_{63} = s_{64} = s_{65} = 0 \tag{6}$$

for some of the components of the matrix $S\,[\boldsymbol{w_g};\ \omega, \Delta x, \Delta y, z_0]$. Further consequences are given by the expressions

$$s_{11}[\boldsymbol{w}_g, \omega, 0{,}0, z_0] = s_{22}[\boldsymbol{w}_g, \omega, 0{,}0, z_0] = s_h[\boldsymbol{w}_g, \omega, z_0] \tag{7}$$

$$s_{33}[\boldsymbol{w}_g, \omega, 0{,}0, z_0] = s_v[\boldsymbol{w}_g, \omega, z_0] \tag{8}$$

where $s_h[\boldsymbol{w}_g;\ \omega, z_0]$ and $s_v[\boldsymbol{w}_g;\ \omega, z_0]$ mean the classical spectrum density characteristics of horizontal and vertical motions at a point of depth z_0 respectively.

In order to postulate analytical expressions for the non-zero components of the coherence matrix, following starting points were accepted:

- the similitude criteria of wave propagation $s_{\Delta\varphi}$ (for phase lag $\Delta\varphi$) and s_θ (for rotation to translation amplitudes), where *c* means a wave propagation speed and *d* means a relative distance (Sandi, 1983):

$$s_{\Delta\varphi} = \frac{c \cdot \Delta\varphi}{\omega \cdot d} \tag{9}$$

$$s_\theta = \frac{c \cdot \theta 0}{\omega \cdot u0} \tag{10}$$

- a space – time similitude assumption of correlation - coherence characteristics, which makes it possible to take the well-known Kanai – Tajimi expressions of correlation – coherence of local motion at a point

$$b\left[\boldsymbol{w}_g{}^{(s)}{}_k(t), t_n, a, \alpha, \beta\right] = a_k^2 exp(-\alpha|t_n|)\{cos(\beta|t_n|) + (\alpha/\beta)sin(\beta|t_n|)\} \tag{11}$$

$$s\left[\boldsymbol{w}_g{}^{(s)}{}_k(t), \omega_m, a, \alpha, \beta\right] = (2a^2/\pi)(\alpha^2+\beta^2)/\{\omega_m^4 + 2(\alpha^2-\beta^2)\omega^2 + (\alpha^2+\beta^2)^2\} \tag{12}$$

as a model in order to specify spatial coherence.

The coherence characteristic for two different points (for illustration, for the first component of the coherence matrix) is postulated as

$$s_{11}[\boldsymbol{w}_g, \omega, \Delta x, \Delta y, z_0] = s_{11}[\boldsymbol{w}_g, \omega, 0{,}0, z_0]\rho\{\upsilon, \omega, T^*(c_p, c_s, \Delta x, \Delta y)\} \tag{13}$$

where the spatial coherence factor $\rho\{\upsilon, \omega, T^*(c_p, c_s, \Delta x, \Delta y)\}$ has the expression

$$\rho(\upsilon, \omega, T^*) = exp(-\upsilon T^*)\{cos(\omega T^*) + (\upsilon/\omega)\, sin\,(\omega T^*)\} \tag{14}$$

while the argument $T^*(c_p, c_s, \Delta x, \Delta y)$, which has a **T** (time) physical dimension, will be

$$T^* = T^*(c_p, c_s, \Delta x, \Delta y) = T_0^*(c_p, c_s, d_l, d_t, z_0) = \{< d_l/c_p(z_0) >^2 + < d_t/c_s(z_0) >^2\}^{1/2} \tag{15}$$

(c_p and c_s mean here conventional wave propagation speeds for *P*- and *S*- waves respectively, while d_l and d_t mean relative distances along corresponding directions).

A first attempt of calibration of the parameter υ was $\upsilon \approx 0.5\ \omega$.

The coherence characteristics concerning rotation components have expressions in which partial derivatives of terms for translation components, with respect to spatial coordinates, intervene.

Given previous developments, the task of calibration of the stochastic ground motion model reduces to that, of calibration of the conventional wave propagation speeds c_p and c_s.

ANNEX II. AN ATTEMPT OF CALIBRATION OF THE PARAMETERS OF THE GROUND MOTION MODEL

A trial and error approach was adopted in order to estimate the most appropriate values for the conventional parameters c_p and c_s. The approach was quite simple and it benefited from the fact that the dominant frequencies of oscillation for ring translation and for ring rotation with respect to its center were very close (see Table 2). The calculations used in this connection are starting from the relation between the vector of acceleration of ground-structure interface, $\boldsymbol{w}_g\ (t)$, and the vector of acceleration along the degrees of freedom of the upper part of the structure, $\boldsymbol{w}_e\ (t)$. One has, for the Fourier images of these two vectors,

$$\overline{\boldsymbol{w}}_e(\omega) = \overline{\boldsymbol{H}}(\omega)\overline{\boldsymbol{w}}_g(\omega) \tag{16}$$

where the non-dimensional transfer function $\boldsymbol{H}^{\sim}(\omega)$ is

$$\overline{\boldsymbol{H}}_{\boldsymbol{gen}}(\omega) = \sum_r \bar{h}_r^{(u)}(\omega)\, \boldsymbol{v}_r \times \boldsymbol{v}_r^T \overline{\boldsymbol{R}}(\omega) \tag{17}$$

$\boldsymbol{v}_r$ are the eigenvectors of *r*-th orders, normalized with respect to the inertia matrix $\boldsymbol{M}$, ”×” means a dyadic product and $h_r^{(u)\,\sim}\ (\omega)$ are the modal transfer functions corresponding to the assumption of a Kelvin – Voigt type constitutive law,

$$\bar{h}_r^{(u)}(\omega) = 1/(\omega_r^2 - \omega^2 + 2i\zeta_r\omega_r\omega) \tag{18}$$

(ω_r: undamped natural circular frequency of r-th order; ζ_r: modal fraction of critical damping) while $\boldsymbol{R}^{\sim}(\omega)$ is the Fourier image of the cross – stiffness matrix of which each column is expressing forces applied along the components of the structural motion vector $\boldsymbol{w}_e^{\sim}(\omega)$, due to unit disturbances along the corresponding components of the ground motion vector $\boldsymbol{w}_g^{\sim}(\omega)$.

In case the acceleration vectors $\boldsymbol{w}_g(t)$ and $\boldsymbol{w}_e(t)$ are assumed to be random, stationary, and are characterized by classical spectrum density matrices $\boldsymbol{S}[\boldsymbol{w}_g;\ \omega]$ and $\boldsymbol{S}[\boldsymbol{w}_e;\ \omega]$ respectively, the deterministic relation (16) leads to the stochastic relation (asterisk means complex conjugate).

$$\boldsymbol{S}[\boldsymbol{w}_e;\omega] = \bar{\boldsymbol{H}}^*(\omega)\,\boldsymbol{S}[\boldsymbol{w}_g;\omega]\bar{\boldsymbol{H}}^T(\omega) \tag{19}$$

The relations given in Section 2 are to be now adapted to the features of the structure, keeping in view appropriate expressions for the horizontal coordinates x_g nd y_g of the columns, as functions of the radius of the infrastructure r_0 and of the azimuthal angles α_i.

The parameters T^* (corresponding to couples of support points characterized by azimuthal angles α_i and α_j) will become

$$T_{1ix}^* = r_0 \times \{< [cos(\alpha_j) - cos(\alpha_i)]/c_l >^2 + < [sin(\alpha_j) - sin(\alpha_i)]/c_t >^2\}^{1/2} \tag{20}$$

$$T_{2ix}^* = r_0 \times \{< [sin(\alpha_j) - sin(\alpha_i)]/c_l >^2 + < [cos(\alpha_j) - cos(\alpha_i)]/c_t >^2\}^{1/2} \tag{21}$$

$$T_{ij}^* = \left({T_{1ij}^*}^2 + {T_{2ij}^*}^2\right)^{1/2} \tag{22}$$

The sum $s_{11ij}[\boldsymbol{w}_g;\ \omega,\ \Delta x_{ij},\ \Delta y_{ij}] + s_{22ij}[\boldsymbol{w}_g;\ \omega,\ \Delta x_{ij},\ \Delta y_{ij}]$, characterizing ground motion will become

$$\begin{aligned} & s_{11_{ij}}[\boldsymbol{w}_g,\omega,\Delta x_{ij},\Delta y_{ij}] + s_{22_{ij}}[\boldsymbol{w}_g,\omega,\Delta x_{ij},\Delta y_{ij}] = \\ & s_h[\boldsymbol{w}_g,\omega] \times < \rho_{ij}[\upsilon,\omega,{T^*}_{1ij}(c_p,c_s,\Delta x_{ij},\Delta y_{ij})] + \rho_{ij}[\upsilon,\omega,{T^*}_{2ij}(c_p,c_s,\Delta x_{ij},\Delta y_{ij})] > \end{aligned} \tag{23}$$

while the function $s^{(s)}[\boldsymbol{w}_e;\ \omega]$, characterizing the motion of the structure, will become

$$\begin{aligned} & s^{(s)}[\boldsymbol{w}_e;\omega] = 1/[(\omega_r^2-\omega^2)^2 + 4{\zeta_r}^2{\omega_r}^2\omega^2] \times (1+\omega^2 T_{rest}^2) \times [\boldsymbol{v}_r \times \boldsymbol{v}_r^T\boldsymbol{R}] \times \\ & \left\{\textstyle\sum_{ij} <\ s_{11_{ij}}[\boldsymbol{w}_g,\omega,\Delta x_{ij},\Delta y_{ij}] + s_{22_{ij}}[\boldsymbol{w}_g,\omega,\Delta x_{ij},\Delta y_{ij}] >\right\} \times [\boldsymbol{R}^T\boldsymbol{v}_r \times \boldsymbol{v}_r^T] \end{aligned} \tag{24}$$

An approximate indicator of modal dynamic magnification to be used in this case is

$$\begin{aligned} & a_r[\boldsymbol{w}_e;\omega] = s^{(s)}[\boldsymbol{w}_e;\omega]/s_h[\boldsymbol{w}_e;\omega] = 1/[(\omega_r^2-\omega^2)^2 + 4{\zeta_r}^2{\omega_r}^2\omega^2] \times (1+\omega^2T_{rest}^2) \times \\ & [\boldsymbol{v}_r \times \boldsymbol{v}_r^T\boldsymbol{R}] \times \left\{\textstyle\sum_{ij} <\ s_{11_{ij}}[\boldsymbol{w}_g,\omega,\Delta x_{ij},\Delta y_{ij}] + s_{22_{ij}}[\boldsymbol{w}_g,\omega,\Delta x_{ij},\Delta y_{ij}] >\right\} \times [\boldsymbol{R}^T\boldsymbol{v}_r \times \boldsymbol{v}_r^T] \end{aligned} \tag{25}$$

T_{ret} means here the retardation time that is specific to the Kelvin – Voigt model, while

$$\zeta_r = \omega_r T_{ret}/2 \tag{26}$$

For one of the trial and error assumptions, one will proceed as follows:

- assume values for the parameters c_p and c_s;
- compare the ratio of values of the ratios $a_r[\boldsymbol{w}_e;\ \omega]$ determined for the translation and overall rotation normal modes respectively with the homologous ratio of peak ordinates of the Fourier spectra;
- option for estimate: the values of c_p and c_s for which best fitting is assumed.

The application of this approach made it possible to develop digital maps of the possible domains of c_p and c_s, as presented in Table 3.

Table 3. Digital map, concerning the allowable domains (in green) for the values c_p and c_s

320	300	280	260	240	220	200		320	300	280	260	240	220	200
550	1.0584	1.1081	1.1877	1.3100	1.4918			550	0.9880	1.0310	1.1015	1.2117	1.3778	
500	1.1192	1.1735	1.2596	1.3917	1.5874	1.8645		500	1.0400	1.0866	1.1626	1.2811	1.4592	1.7155
480	1.1492	1.2057	1.2951	1.4319	1.6344	1.9207		480	1.0656	1.1141	1.1928	1.3153	1.4992	1.7638
460	1.1833	1.2424	1.3355	1.4777	1.6877	1.9842		460	1.0947	1.1453	1.2271	1.3541	1.5447	1.8185
440	1.2224	1.2844	1.3817	1.5299	1.7485	2.0562		440	1.1281	1.1810	1.2663	1.3986	1.5967	1.8808
420	1.2674	1.3327	1.4348	1.5899	1.8181	2.1384		420	1.1665	1.2222	1.3115	1.4497	1.6564	1.9522
400	1.3197	1.3887	1.4963	1.6592	1.8981	2.2322		400	1.2111	1.2699	1.3639	1.5089	1.7252	2.0342
380	1.3806	1.4541	1.5679	1.7396	1.9904	2.3395		380	1.2631	1.3257	1.4251	1.5779	1.8052	2.1288
360	1.4524	1.5308	1.6518	1.8334	2.0974	2.4623		360	1.3244	1.3913	1.4969	1.6587	1.8985	2.2384
340		1.6215	1.7506	1.9432	2.2213	2.6024		340		1.4691	1.5819	1.7540	2.0078	2.3654
320			1.8674	2.0719	2.3646	2.7607		320			1.6832	1.8668	2.1362	2.5123

REFERENCES

Lederer F (1961) “Gitterschalen aus Stahlrohren”, *Shell Research, Proceedings of the Symposium on Shell Research*, Delft, August 30-September 2 1961, North-Holland Publishing Company, Amsterdam

Murzea P (2012) Studiu asupra specificarii marimilor de intrare privind actiunea seismica asupra constructiilor, Ph.D Thesis, Technical University of Civil Engineering, Bucharest, Romania

Murzea P, Sandi H, Vlad I, Vlad MN (2013) “Calibration of a Ground Motion Model, Using Full Scale Experimental Data on Ambient Vibration”, *Buletin of the Transilvania University of Braşov*, Vol. x (xx) – 2013, Series I

Murzea P, Sandi H, Vlad I, Vlad MN (2013) “An attempt of calibration of a stochastic model of low amplitude stationary ground motion”, *Session of the Commission of Acoustics of the Romanian Academy*, Bucharest

Sandi H (1983) Elemente de dinamica structurilor (Elements of structural dynamics) . Editura Tehnică, Bucharest

Sandi H, Stancu M, Stancu O, Borcia IS (1986) “A biography of a large-span structure, pre- and post-earthquake, after the provisional and final strengthening”. *Proc. 8-th European Conf. on Earthquake Engineering*, Lisbon

Soare MV (1963) “The metallic lattice dome of the National Economy Exhibition Pavilion at Bucharest” in *Hanging roofs*. North Holland Publisher Company, Amsterdam

Vlad I and Vlad M (2014) “Structural identification and vibration problems in buildings with dome roofs”**,** *Proceedings of the 10th National Conference in Earthquake Engineering*, Earthquake Engineering Research Institute, Anchorage, Alaska

Sandi H (2005) “On the seismic input for the analysis of irregular structures*”, Proc. IASS Annual Symp. “IASS 2005 – Theory, Technique, Valuation, Maintenance*” Bucharest